



HAL
open science

Photochemical interactions between pesticides and plant volatiles

Yara Arbid, Mohamad Sleiman, Claire Richard

► **To cite this version:**

Yara Arbid, Mohamad Sleiman, Claire Richard. Photochemical interactions between pesticides and plant volatiles. *Science of the Total Environment*, 2022, 807, pp.150716. 10.1016/j.scitotenv.2021.150716 . hal-03383730

HAL Id: hal-03383730

<https://hal.science/hal-03383730>

Submitted on 18 Oct 2021

HAL is a multi-disciplinary open access archive for the deposit and dissemination of scientific research documents, whether they are published or not. The documents may come from teaching and research institutions in France or abroad, or from public or private research centers.

L'archive ouverte pluridisciplinaire **HAL**, est destinée au dépôt et à la diffusion de documents scientifiques de niveau recherche, publiés ou non, émanant des établissements d'enseignement et de recherche français ou étrangers, des laboratoires publics ou privés.

1 **Photochemical interactions between pesticides and plant volatiles**

2
3 Yara Arbid, Mohamad Sleiman, Claire Richard*

4 Université Clermont Auvergne, CNRS, ICCF, F-63000 Clermont-ferrand, FRANCE

5
6 **Abstract** : Among the numerous studies devoted to the photodegradation of pesticides, very
7 scarce are those investigating the effect of plant volatiles. Yet, pesticides can be in contact
8 with plant volatiles after having been spread on crops or when they are transported in surface
9 water, making interactions between the two kind of chemicals possible. The objectives of the
10 present study were to investigate the reactions occurring on plants. We selected thyme as a
11 plant because it is used in green roofs and two pesticides : the fungicide chlorothalonil for its
12 very oxidant excited state and the insecticide imidacloprid for its ability to release the radical
13 NO₂ under irradiation. Pesticides were irradiated with simulated solar light first in a solvent
14 ensuring a high solubility of pesticides and plant volatiles, and then directly on thyme's
15 leaves. Analyses were conducted by headspace gas chromatography-mass spectrometry (HS-
16 GC-MS), GC-MS and liquid chromatography-high resolution mass spectrometry (LC-
17 HRMS). In acetonitrile, chlorothalonil photosensitized the degradation of thymol, α -pinene,
18 3-carene and linalool with high quantum yields ranging from 0.35 to 0.04, and was
19 photoreduced, while thymol underwent oxidation, chlorination and dimerization. On thyme's
20 leave, chlorothalonil was photoreduced again and products arising from oxidation and
21 dimerization of thymol were detected. Imidacloprid photooxidized and photonitrated thymol
22 in acetonitrile, converting it into chemicals of particular concern. Some of these chemicals
23 were also found when imidacloprid was irradiated dispersed on thyme's leaves. These results
24 show that photochemical reactions between pesticides and the plants secondary metabolites

25 can take place in solution as on plants. These findings demonstrate the importance to increase
26 our knowledge on these complex scenarios that concern all the environmental compartments.

27 **Key-words** : Chlorothalonil, imidacloprid, thyme's leaves, photoreduction, photooxidation,
28 photonitration

29

30 **Introduction**

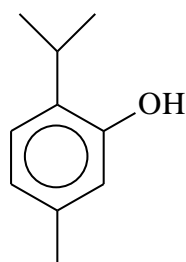
31 Pesticides undergo degradation processes in surface waters (Pehkonen and Zhang,
32 2002), on the surface of soil and of leaves (Katagi, 2004) yielding breakdown chemicals. The
33 potential effects of these chemicals on wildlife and human health have attracted numerous
34 studies aiming for identification and to improve knowledge on their physico-chemical,
35 biological and toxicological properties (Martínez Vidal et al., 2019, de Souza et al., 2020).

36 Pesticides are generally photodegraded when they absorb solar light (Burrows et al.,
37 2002, Mathon et al., 2021) or when they are irradiated in the presence of natural
38 chromophoric species acting as sensitizers (natural organic matter) or photoinducers (nitrate
39 ions, ferric species...) (Remucal, 2014, Ossola et al., 2021, Marussi and Vione, 2021, Brand
40 et al., 1998). Photochemical reactions between two pesticides can also take place. In our
41 group, we have demonstrated that mixing mesotrione and nicosulfuron (Ter Halle et al., 2010)
42 or chlorothalonil and cycloxydim (Monadjemi et al., 2011) enhances the rate of
43 photodegradation of each of them. Thiophanate-methyl was also shown to favor the
44 photodegradation of methyl-bifenazate (Hamdache et al., 2018). These results were explained
45 by the capacity of chlorothalonil and the primary photoproduct of thiophanate-methyl to
46 generate oxidant triplet excited states and singlet oxygen capable of oxidizing other
47 pesticides. In addition, reactions can be drastically affected by the medium. This was
48 illustrated in the case of the insecticide methyl-bifenazate, the photodegradation of which was
49 measured to be 70-fold faster on green pepper skin than on a film of paraffinic wax
50 (Hamdache et al., 2018). This behaviour was rationalized by the presence of water from
51 pepper. These results bring evidence that the fate of pesticides can be affected by the presence
52 of other chemicals present in the medium apart from the well-known sensitizers or
53 photoinducers.

54 Volatile compounds emitted by plants are the subject of intense research because of
55 their implication in atmospheric chemistry, air pollution and defense of plants against
56 pathogens (Atkinson and Arey 2003, Mellouki et al 2015, Wannaz et al, 2003, Hammerbacher
57 et al, 2019). However, to the best of our knowledge, scenarios in which they could interact
58 with pesticides were rarely considered in the literature. These potential reactions concern all
59 the environmental compartments. When a pesticide is dispersed on the crop leaves just after
60 been applied, it is surrounded by plant's volatiles facilitating reactions between each group of
61 chemicals at the solid gas interface. Moreover, pesticides and plant volatiles can be
62 transported to surface water after their solubilization in the run off water and can interact in
63 the aquatic compartment. Plant volatiles correspond to a large group of chemicals : mono, di
64 and triterpenes/terpenoids, phenols (Dudareva 2006, Abbas et al 2017, Mochizuki et al, 2020).
65 They bear functionalities such as H-atoms, double bonds and aromatic rings giving them
66 possibilities to be involved in a lot of photochemical reactions.

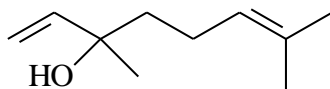
67 Here, we investigated the photochemical reactivity of two pesticides : the fungicide
68 chlorothalonil (CT) and the insecticide imidacloprid (IMD) in the presence of the main thyme
69 volatiles : thymol (T), linalool, 3-carene, α -pinene. These terpenes and thymol are common to
70 other plant species (Carretero et al 2018). Both pesticides are susceptible to have an effect on
71 the plant volatiles : CT shows photooxidant properties via its triplet excited state or the
72 formation of singlet oxygen ($^1\text{O}_2$) (Ter Halle 2010) while IMD releases NO and NO₂ under
73 irradiation making it a potential nitrosating/nitrating agent (Palma et al 2020). Out of nitrogen
74 oxides, NO and NO₂ are considered toxic (Skalska et al., 2010). Experiments were first
75 conducted in solution to evidence the reactions. Acetonitrile was chosen for its ability to
76 ensure a high solubility of all the studied chemicals. Then, pesticides were directly irradiated
77 on leaves of thyme to approach the real conditions closely.

78

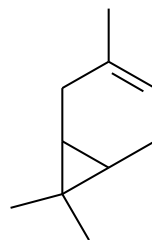


79

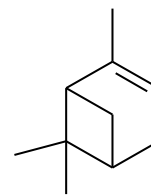
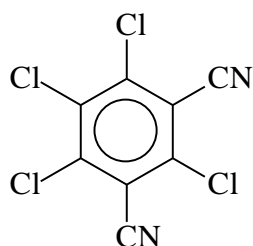
80 T



Linalool



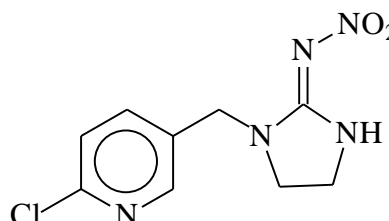
3-Carene

 α -Pinene

81

82

CT



IMD

83

84 Scheme 1 : Structure of chlorothalonil (CT), imidacloprid (IMD), thymol (T), linalool, 3-
85 carene and α -pinene

86

87 Experimental part

88 **Chemicals and standards.** IMD ($C_9H_{10}ClN_5O_2$) and CT ($C_8Cl_4N_2$) were purchased from
89 Sigma Aldrich (PestanalTM, analytical standard, $\geq 98.0\%$). T ($C_{10}H_{14}O$, $\geq 98.5\%$), α -pinene
90 ($C_{10}H_{16}$, 98%), 3-carene ($C_{10}H_{16}$, 90%), linalool ($C_{10}H_{18}O$, $\geq 97.0\%$ GC area %),
91 thymoquinone (TQ, $C_{10}H_{12}O_2$, $\geq 98\%$) were all purchased from Sigma Aldrich.
92 Thymohydroquinone (TQH₂, $C_{10}H_{14}O_2$, 95%) was purchased from Enamine, Ukraine. All
93 were used without further purification. Water was produced using a reverse osmosis RIOS 5
94 and Synergy (Millipore) device (resistivity 18 M Ω cm, DOC < 0.1 mg L⁻¹). Acetonitrile
95 (ACN) was purchased from Carlo Erba Reagents (HPLC Plus Gradient grade-ACS-Reag).
96 Thyme (*Thymus Vulgaris*) was freely grown under natural sunlight in a garden for seven years

97 in Beaumont (France) and regularly watered. In the case of IMD, we undertook a comparative
98 set of experiments on a thyme plant (*Thymus Vulgaris*) bought in a garden center.

99 **Samples preparation.** All stock solutions were prepared in ACN and kept in the dark at 4°C
100 before use. Final solutions were prepared by diluting stock solutions with ACN. For the
101 experiments on thyme leaves, twigs were cut using scissors. Each twig contained 30 leaves
102 (average area of each leave of 0.03 cm²) for a total area of 1.8 cm² considering the two faces.
103 Twigs were dipped in IMD or CT solution (7.5×10⁻⁴ M) for 30 s, left to dry freely for an hour,
104 and then put in hermetically sealed headspace (HS) vials to be either used for control
105 experiments in the dark or irradiated. Dark controls in the absence of pesticides were
106 conducted with twigs directly put in HS vials. The surface concentration of IMD and CT on
107 twigs was evaluated as follows : twigs covered by CT were immersed and agitated in 2 mL of
108 acetonitrile for 2 min while those covered by IMD in 5 mL of acetonitrile. Solutions were
109 then analyzed by high performance liquid chromatography coupled to a photodiode-array
110 detector(HPLC-DAD) to determine the CT's and IMD's concentrations.

111 **Irradiation.** Solar UV radiations reaching the earth's surface contain UVA (315-400 nm) and
112 a part of UVB (295-315 nm). The absorption spectrum of CT and IMD overlapping the
113 radiations reaching the earth's surface within the wavelength range 295-350 nm (Figure SI-
114 1A), we used the following irradiation devices to simulate solar light. The first one (device 1)
115 was used to calculate the quantum yield of CT photodegradation in the presence of thyme's
116 volatiles. Solutions containing CT (10⁻⁴ M) + volatiles (10⁻³ M) were put in a cuvette and
117 irradiated at 313 nm (UVB) in parallel beam using a high pressure mercury lamp equipped
118 with an Oriel monochromator. A radiometer QE65000 from Ocean optics was used to
119 measure the photon flux I₀: (3.0±0.2)×10¹⁴ photons cm⁻² s⁻¹ at 313 nm. Samples were taken at
120 chosen irradiation times and directly analyzed by HPLC-DAD to follow the degradation
121 profile of CT. To monitor the disappearance of CT or IMD (10⁻⁴ M) in ACN alone or in the

122 presence of volatiles (10^{-3} M) and detect new photoproducts we needed to use a device
123 delivering a more intense photon flux. Solutions (20 ml) were placed in a cylindrical Pyrex
124 reactor (1.4 cm internal diameter) sealed with an air-tight silicon cap surrounded by 3
125 polychromatic tubes simulating UVB (Philips, TL20W/01-RS, $\lambda_{\max} = 313$ nm) installed inside
126 a custom-made cylindrical irradiation device (device 2). Aliquots were sampled at chosen
127 irradiation times and directly analyzed by HPLC-DAD to monitor the degradation profiles of
128 CT or IMD and UHPLC coupled to high resolution mass spectrometry (LC-HRMS) and gas
129 chromatography coupled to mass spectrometry (GC-MS) to identify photoproducts. The third
130 device (device 3) was a solar simulator CPS Atlas equipped with a xenon arc lamp, a filter
131 cutting off wavelengths shorter than 290 nm and a cooling system maintaining the bottom of
132 the device at 10°C. The global irradiance in the range of 300-800 nm was set at 500 W m⁻². It
133 represents a medium value at 40°N latitude in summer. This device was used to irradiate the
134 HS vials containing thyme twigs alone or covered with IMD or CT. In the case of IMD, 2 h of
135 irradiation were enough to detect significant amounts of nitro derivatives of thymol. For CT,
136 due to the difficulty to demonstrate the interaction between CT and thyme's volatile, we
137 extended the irradiation until 6 h. Vials were then analyzed directly by Headspace gas
138 chromatography coupled to mass spectrometry (HS-GC-MS) or chemicals contained in and
139 on twigs were extracted by ACN as previously explained and analyzed by LC-HRMS or GC-
140 MS. Irradiation experiments in solution were duplicated and on twigs duplicated or
141 triplicated.

142 **Analyses.** UV-Vis absorption spectra of volatiles, CT, IMD, TQ, and TQH₂ were recorded
143 using a Varian Cary 3 spectrophotometer. CT and IMD degradation profiles were tracked by
144 HPLC-DAD using a NEXERA XR HPLC-DAD apparatus. The analytical column was a
145 Phenomenex-kinetex C₁₈ (100 mm×2.1 mm, 2.6 μm particle size) for CT experiments and EC
146 150/4.6 NUCLEODUR C₁₈ endcapped column for IMD analyses. The eluent was a mixture of

147 ACN and water and the flow rate was set at 0.2 and 1 mL min⁻¹ for CT and IMD,
148 respectively. The HPLC conditions for CT were as follows: the elution gradient started with
149 30% ACN maintained for 2 min and then linearly increased to reach 80% after 13 min; while
150 that for IMD started with 30% ACN which was maintained for 10 min. Photoproducts were
151 analyzed and quantified using HRMS on an Orbitrap Q-Exactive (ThermoScientific) coupled
152 to an ultra-high performance liquid chromatography (UHPLC) instrument Ultimate 3000
153 RSLC (ThermoScientific). The column was a Kinetec EVO C₁₈ (100×2.1 mm), particle size of
154 1.7 μm (Phenomenex). The elution gradient started with 15% acetonitrile maintained for 5
155 min, then the percentage of acetonitrile was linearly increased to reach 55% after 5 min. The
156 flow was set at 0.45 mL min⁻¹. Analyses were made in positive (ESI⁺/ESI) electrospray
157 mode. Identification of the major constituents was carried out using the Xcalibur software and
158 when necessary by matching retention times with those of authentic standards. The m/z of
159 proposed structures differed by less than 5 ppm from the theoretical mass. Standard solutions
160 of TQ were analyzed immediately after have been prepared. The limit of detection LOD in the
161 case of TQ was estimated to 10⁻⁶ M by analyses of authentic solutions.

162 Photoproducts were also analyzed using an Agilent 6890 GC coupled to an Agilent 5973 MS.
163 The separation was carried out using a HP-5 μs column (25 m×0.25 mm×0.25 μm) operating
164 initially at 80°C over 1 min, followed by a 10°C min⁻¹ ramp to reach 200°C and then a 30⁰ C
165 min⁻¹ ramp to reach 260°C maintained for 1 min (to calculate the degradation of terpenes) in
166 the case of CT experiments, while the analysis was operated initially at 70°C followed by a
167 10°C min⁻¹ ramp to reach 160°C for 5 min and then a 30°C min⁻¹ ramp to reach 250°C
168 maintained for 2 min in the case of IMD. The flow rate was 1 mL.min⁻¹ with an injection
169 volume of 1 μL in both cases. T and some of its photoproducts were quantified after
170 derivatization with N,O-Bis (trimethylsilyl)trifluoroacetamide (BSTFA). The derivatizing

171 solution (2 mL) was prepared by mixing 60 μ L of BSTFA with 1.4 mL sample. Separation
172 was achieved as previously described for CT experiments.

173 To determine the volatile metabolites produced by the plant, HS-GC-MS (Shimadzu HS-20
174 coupled with QP2010SE) was used. Twigs of 0.2 g alone or after dipping in CT solution were
175 transferred into a 20 mL headspace glass vial, then left in the dark or irradiated and incubated
176 for 5 min at 80⁰ C. The analytical column (Mega 5-MS 30 m \times 0.25 mm) was operated
177 initially at 50⁰C for 1 min, followed by an 8⁰C min⁻¹ ramp to reach 170⁰C and held for 4 min,
178 and then a 15⁰C min⁻¹ ramp to reach 275⁰C maintained for 1 min. The mass spectrometer
179 source was heated to 200⁰C, and signals were detected between mass to charge ratios (m/z) of
180 50 and 350.

181 Identification of the major constituents was carried out using the NIST 17 database and when
182 necessary by matching retention times and ion fragments with those of authentic standards.
183 For calibration, a stock solution of T was prepared in ethanol at a concentration of 1 g L⁻¹.
184 Quantification of T was performed by means of 5-point calibration curve for which the
185 concentrations of standards ranged from 2-100 mg L⁻¹. All standard solutions were stored in
186 dark at 2-8⁰C in amber glass vials with Teflon-lined caps. They were found to be stable under
187 short-term (48 h) storage conditions. A linear response was obtained with a correlation
188 coefficient (R²) of 0.997. Selectivity was evaluated by analyzing a set of blank samples and
189 monitoring the absence of interferences with S/N ratios higher than 3. No significant
190 interfering peaks were observed in the ion chromatogram time window monitored for T. The
191 precision of the method was determined by calculating the relative standard deviation (RSD)
192 of six replicate measurements of diluted T solution (10 mg L⁻¹). All RSDs were acceptable
193 and less than 7% indicating a good precision. The limit of detection LOD was calculated from
194 the standard deviation (σ) of multiple measurements (n=7) of diluted T solutions within a
195 factor of 5 of the background signal. LOD was set equal to 3 σ which resulted in a value of 13

196 pg. The Limit of quantification (LOQ) was defined as 10σ or 43 μg . In all cases, LOD and
197 LOQ were significantly below the levels determined in the thyme extracts (0.07 to 2.7 mg).

198

199 **Quantum yields of CT photodegradation in the presence of terpenes in acetonitrile.** The
200 quantum yield of CT photodegradation (Φ_{CT}) was determined using **Eq 1**:

201 $\Phi_{\text{CT}} = \Delta c / (I_a \times \Delta t)$ **Eq 1**

202 where $\Delta c / \Delta t$ was the rate of CT consumption expressed in M s^{-1} and I_a was the rate of photon
203 absorption by CT at 313 nm expressed in Einstein $\text{L}^{-1} \text{s}^{-1}$. I_a was obtained using **Eq 2**:

204 $I_a = I_0 \times (1 - 10^{-\varepsilon \times \ell \times [\text{CT}]_0}) \times 1000 / \ell$ **Eq 2**

205 where $\varepsilon = 1760 \text{ M}^{-1} \text{ cm}^{-1}$, $[\text{CT}]_0 = 10^{-4} \text{ M}$, and $\ell = 1 \text{ cm}$.

206 **Laser flash photolysis.** Laser flash photolysis experiments were carried out using an Applied
207 Photophysics LKS.60 apparatus equipped with a Nd^{3+} :YAG laser Quanta-Ray GCR-130 used
208 in a right-angle geometry with respect to the monitoring light beam. Samples were irradiated
209 using the fourth harmonic (266 nm, 9 ns pulse duration) in a quartz cuvette. $^3\text{CT}^*$ was
210 generated by irradiating CT ($5 \times 10^{-5} \text{ M}$ in aerated ACN) and its decay monitored at 330 nm.
211 The reactivity of $^3\text{CT}^*$ with thyme's volatiles was measured within the concentration range
212 $10^{-4} - 2 \times 10^{-3} \text{ M}$. In the case of IMD, no transient species were detected.

213 **Photoproducts toxicity.** The toxicity of photoproducts formed during the irradiations was
214 estimated using the **freely available** ECOSAR (ECOLOGICAL Structure-Activity Relationship)
215 computer program (v 2.0). It predicts the toxicity of a molecule using a structure-activity
216 approach. The acute (LC50, the concentration that is lethal to half of fish after 96 h of
217 exposure to a certain molecule) and chronic toxicities (ChV) of CT, IMD, and formed
218 photoproducts on fish in fresh waters as well as $\log K_{ow}$ were obtained. The program (v 2.0)
219 is available from the website: epa.gov/tsca-screening-tools/ecological-structure-activity-relationships-ecosar-predictive-model.
220

221
222
223
224
225
226
227
228
229
230
231
232
233
234
235
236
237
238
239
240
241
242
243
244
245

Results

1. Characterization of the thyme's constituents

This first objective was to determine what are the main volatile compounds in thyme's twigs, to estimate the amount of T in thyme's twig and to identify and quantify the chemicals related to T. Volatile compounds released from thyme's twigs after two hours in the dark in the HS vials were analyzed by HS-GC-MS (Figure SI-2). T, linalool, 3-carene and α -pinene were the main detected compounds. T is a phenolic compound while linalool, 3-carene and α -pinene are terpenes (Scheme 1). The amount of extractable T from thyme's twigs by ACN was measured by GC-MS. Based on several replicates using twigs containing 30 leaves (weight 0.2 g), it could be estimated to range between 0.35 and 2.7 mg per g of wet twigs. After that, we analyzed the non-volatile chemicals. For this, two vials containing two twigs each were left in the dark for 4h, extracted in 2 ml of ACN and analyzed by UHPLC-HR-MS and GC-MS. Several peaks directly connected to T were found (Table 1). By UHPLC-HR-MS, one got a peak at $m/z = 165.0901$ in ES^- corresponding to $[M+O-H^+]^-$ and named TO. By MS-MS, TO gave two main fragments at 149.0593 and 135.0443 corresponding to the loss of O and CH_2O , respectively (Figure SI-3). The oxidation of T can take place on the isopropyl group, on the methyl group or on the ring. No loss of H_2O was observed ruling out an oxidation of the isopropyl carbon atoms. The oxidation of the ring would lead to thymolhydroquinone. However, TO was not assigned to thymolhydroquinone because the two compounds had different retention times in HPLC (3.3 min for TO against 4.5 min for thymolhydroquinone), and different maximum of absorption (278 nm for TO against 290 nm for thymolhydroquinone). We therefore concluded that TO was the benzyl alcohol derivative (Table 1). The peak detected at $m/z = 165.0901$ in ES^+ (Figure SI-4) corresponded to $[M+O-$

246 $2\text{H}+\text{H}^+]^+$ and was assigned to the quinonic derivative TQ (Table 1). Its maximum of
247 absorption at 250 nm was fully in line with this assignement. The other peak at $m/z =$
248 179.0704 in ES^- corresponding to $[\text{M}+2\text{O}-2\text{H}-\text{H}^+]^-$ was attributed to the quinonic derivative of
249 TO, TQO (Figure SI-5). The two peaks showing $m/z = 313.1806$ and 329.1754 in ES^- were
250 assigned to dimers, T-TO- $_{2\text{H}}$ and TO-TO- $_{2\text{H}}$, respectively (Figures SI-6 and 7). By GC-MS,
251 TO, TQ and several isomers of TO-TO- $_{2\text{H}}$ were also detected.

252 The second objective was to investigate the effect of irradiation on the formation of
253 these compounds. For this, two vials containing two twigs each were irradiated in the solar
254 simulator for 4h and extracted using ACN. The same compounds were detected and the effect
255 of irradiation on their formation can be seen in Table 2. The peak areas were between 15 and
256 100-fold higher after irradiation than in the dark showing the drastic effect of light.

257

258 **2. Interactions between CT and thyme's volatiles**

259 **2.1. Irradiation of CT and thyme's volatiles in acetonitrile solution**

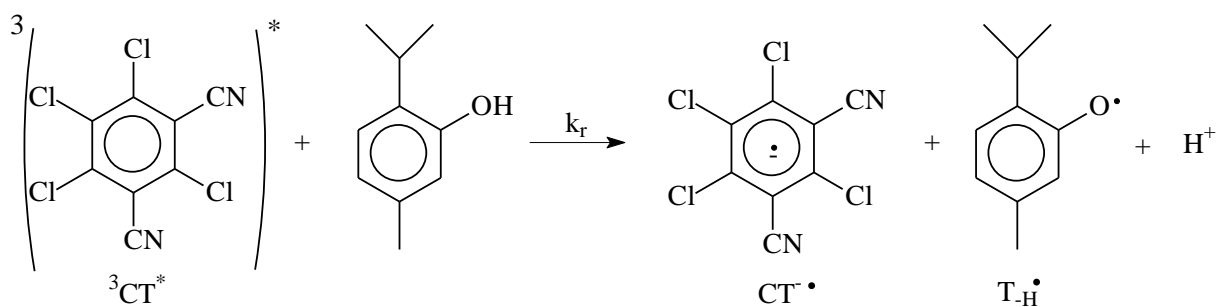
260 Neither T, 3-carene, linalool and α -pinene nor CT underwent significant photodegradation
261 when irradiated alone in ACN solution. Thyme's volatiles do not absorb the radiations
262 emitted by the tubes (Figure SI-1B), while CT absorbs the radiations (Figure SI-1A) but
263 yields a triplet excited state $^3\text{CT}^*$ efficiently deactivated by oxygen ($7.8 \times 10^8 \text{ M}^{-1} \text{ s}^{-1}$,
264 Monadjemi et al., 2011) (Figure 1A). In contrast, the irradiation of CT (10^{-4} M) in the
265 presence of each of these volatiles (10^{-3} M) led to the fast disappearance of CT (Figure 1A)
266 and the thyme's volatiles (Figure 1B). As shown in Figure 1A, the CT photodegradation
267 increased in the order $\text{T} > \alpha\text{-pinene} > 3\text{-carene} > \text{linalool}$. In accordance, the quantum yield of
268 CT photodegradation (Φ_{CT}) was equal to 0.35, 0.20, 0.15, 0.04 for T, α -pinene, 3-carene and
269 linalool, respectively against < 0.001 for CT alone. Concerning the thyme's volatiles loss, T
270 was the fastest to disappear, followed by α -pinene, 3-carene, and linalool (Figure 1B).

271

272

273 To confirm the ability of thyme's volatiles to react with $^3\text{CT}^*$ and measure the
274 bimolecular rate constant of the reaction (k_r), we undertook laser flash photolysis
275 experiments. CT was irradiated in the presence of each of these chemicals added at a
276 concentration comprised between 3×10^{-4} and 2×10^{-3} M while the decay of $^3\text{CT}^*$ was
277 monitored at 330 nm (Figure 2). Alone, in air-saturated ACN, $^3\text{CT}^*$ disappeared by an
278 apparent first order kinetic with $k = 1.6 \times 10^6 \text{ s}^{-1}$ corresponding to the sum $k_d + k_{\text{O}_2}[\text{O}_2]$, where
279 k_d is the rate constant of **deactivation** by collision with the solvent molecules, k_{O_2} the rate
280 constant of reaction with oxygen and $[\text{O}_2]$ the concentration of oxygen in the solution. In the
281 presence of T, $^3\text{CT}^*$ disappeared faster than alone showing that a reaction between $^3\text{CT}^*$ and
282 T took place (Figure 2A). This reaction might be an energy transfer or an electron/H atom
283 transfer reaction. The energy level of $^3\text{CT}^*$ was previously estimated to lay at 275 kJ mol^{-1}
284 based on phosphorescence measurements at 77 K in pentane (Porrás et al, 2014). This is lower
285 than the energy level reported for phenol $\sim 314\text{-}334 \text{ kJ.mol}^{-1}$ (Becker, 1969) making the
286 energy transfer from $^3\text{CT}^*$ to T unlikely. Moreover, given the ability of $^3\text{CT}^*$ to oxidize
287 phenols (Monadjemi et al., 2011), an electron or H atom transfer from T to $^3\text{CT}^*$ with
288 formation of the reduced CT radical ($\text{CT}^{\cdot-}/\text{CTH}^{\cdot}$) and the phenoxyl radical ($\text{T}_{\cdot\text{H}}$) (Scheme 2)
289 looks more probable .

290



291

292

Scheme 2 : Reaction of $^3\text{CT}^*$ with thymol

293

294 The shape of the time-resolved absorption spectrum of Figure 3A revealed the

295 formation of a secondary species that could be therefore either the reduced CT radical or T-H^\bullet .

296 Its significant absorption measured at 330 nm matches more with the reduced CT radical

297 (Bouchama et al., 2014) than with T-H^\bullet that shows maxima at 390 and 410 nm (Venu et al.,

298 2013). Due to the overlapping of the two species absorption, a numerical analysis of the

299 differential equations was necessary to determine the k_r value. The best fit of the experimental

300 data was obtained by taking $k_r = 7.0 \times 10^9 \text{ M}^{-1} \text{ s}^{-1}$, $\epsilon_{\text{CT}^*} / \epsilon_{\text{phenoxy}} = 2.0$, and a first order decay

301 rate constant of $5 \times 10^5 \text{ s}^{-1}$ for the reduced CT radical in air-saturated medium (Monadjemi et

302 al., 2014). Individual evolution of these species are shown in the inset of Figure 2A.

303

304 In the case of α -pinene, 3-carene and linalool, the absorbance at 330 nm completely

305 decayed within 1 μs following the flash (Figure 2B). This result demonstrated the reaction of

306 $^3\text{CT}^*$ with terpenes. However, with these compounds, the formation of the reduced CT radical

307 was not observed (Figure 2B). Values of k_r could be deduced from the linear plot of k , the

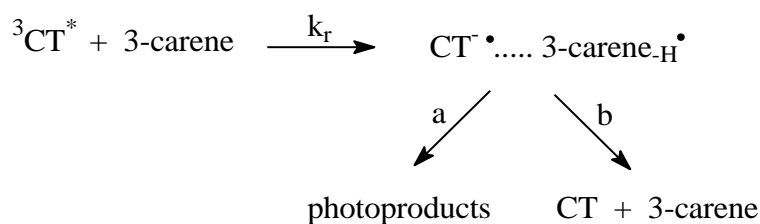
308 observed first order rate constant, vs [terpene] (inset of Figure 2B). Assuming $k = k_d +$

309 $k_{\text{O}_2}[\text{O}_2] + k_r[\text{terpene}]$, one got $k_r = 2.6 \times 10^9$, 2.8×10^9 and $3.9 \times 10^9 \text{ M}^{-1} \text{ s}^{-1}$ for α -pinene, 3-

310 carene, and linalool, respectively. The oxidation of terpenes by $^3\text{CT}^*$ was likely due to the

311 presence of labile H atoms in their structures and the non-observation of the 330 nm radical
 312 could be tentatively explained by an in-cage reaction between the reduced CT radical and the
 313 oxidized terpene radical leading directly to photoproducts (Scheme 3 in the case of 3-carene).
 314 If one admits that the relative importance of process **a** that yielded photoproducts and process
 315 **b** in which CT was regenerated depended on the structure of the terpene, then one can also
 316 explain why Φ_{CT} varied from 0.20 for α -pinene to 0.04 for linalool whereas the k_r values laid
 317 in a very narrow range for these two compounds. Finally, we found that all four thyme's
 318 volatiles readily reacted with $^3CT^*$. The higher reactivity of T compared to that of α -pinene,
 319 3-carene, and linalool is in line with the presence of an easily abstractable phenolic H atom.

320



321

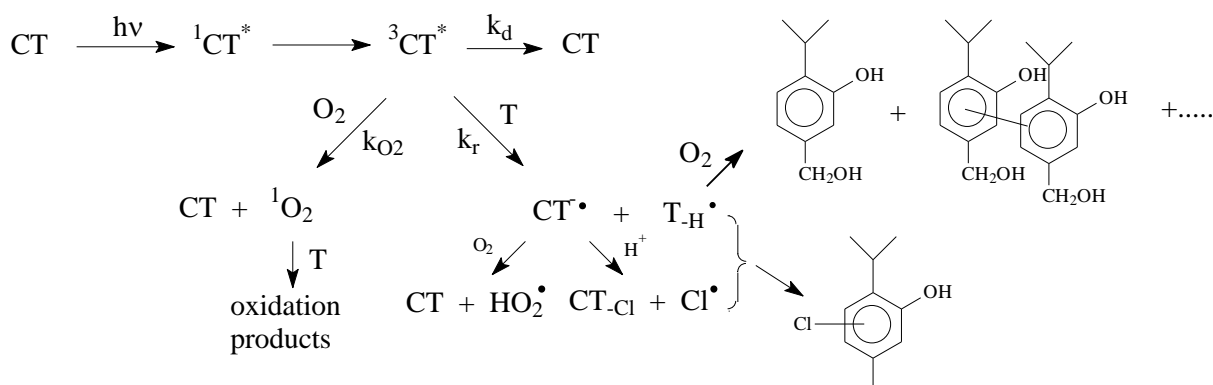
322

323 Scheme 3 : Reaction of $^3CT^*$ with 3-carene

324

325 Product studies was also undertaken by GC-MS and UHPLC-HRMS . For the CT+T
 326 mixture, we detected a new photoproduct showing $m/z = 183.0571$ and 185.0542 in ES^- along
 327 with TO, TQ, TQO, T-TO_{2H} and TO-TO_{2H}. This compound corresponded to $[T-H+Cl-H^+]$
 328 and was named TCl (Table 1). By GC-MS, we detected TCl again, CT_{Cl} and CT_{2Cl}. The
 329 formation of dechlorinated CT confirmed that photoreduction took place. CT_{Cl} was also
 330 detected upon the irradiation of CT+3-carene, but no other photoproducts were found by GC-
 331 MS and no photoproducts at all were detected with α -pinene and linalool.

332 Based on these data and on the known CT photoreactivity, the reaction pathways
 333 shown in Scheme 4 can be proposed to explain the reaction between CT and T. In neat
 334 acetonitrile, $^3\text{CT}^*$ is generated with a quantum yield close to unity and trapped by O_2 ($k_{\text{O}_2} =$
 335 $(1 \pm 0.1) \times 10^9 \text{ M}^{-1} \text{ s}^{-1}$) to yield $^1\text{O}_2$ with a quantum yield equal to 0.85 ± 0.06 (Bouchama et al,
 336 2014). T will therefore compete with O_2 for the reaction with $^3\text{CT}^*$. Taking $k_r = 7.0 \times 10^9 \text{ M}^{-1}$
 337 s^{-1} and $[\text{O}_2] = 1.9 \times 10^{-3} \text{ M}$ in air-saturated acetonitrile solution at 24°C (Murov et al, 1993),
 338 one can estimate that T (10^{-3} M) could trap 79% of $^3\text{CT}^*$ while 21% of O_2 . In our
 339 experimental conditions, T was thus mainly photooxidized through a direct reaction with
 340 $^3\text{CT}^*$, however, given the known good reactivity of singlet oxygen with phenolic compounds
 341 (Wilkinson and Brummer, 1981), a part of the loss of T may be attributable to the reaction $\text{T} +$
 342 $^1\text{O}_2$. Once formed, $\text{T}_{\cdot\text{H}}$ should be further oxidized into TO, TQ and yield dimeric species. The
 343 detection of TCl demonstrates that CT can also photoinduce the chlorination of other
 344 chemicals. A possible explanation is the release of chlorine atoms from CT^{\cdot} followed by their
 345 recombination with $\text{T}_{\cdot\text{H}}$ (Scheme 4). Such a reaction also rationalizes the formation of
 346 dechlorinated CT.



347
 348

349 Scheme 4: Mechanism of CT photolysis in the presence of T

350

351 The values of k_r for terpenes were 1.8 to 2.7-fold lower than for T. Therefore, the
352 percentage of $^3\text{CT}^*$ trapped by terpenes at 10^{-3} M should be consequently lower than for T
353 and the amount of singlet oxygen generated higher. The photooxygenation of terpenes bearing
354 double bonds such as α -pinene, linalool and 3-carene is therefore likely in our conditions,
355 given their reactivity with singlet oxygen (Chiron et al, 1997).

356 Similar reactions can take place in water or in media enriched in water because $^3\text{CT}^*$
357 was also detected in water/acetonitrile (90 :10, v/v) with a quantum yield of formation also
358 close to unity (Bouchama et al, 2014). However, changing the solvent is expected to induce
359 some changes in the pathway ratios. For instance, the percentage of $^3\text{CT}^*$ trapped by O_2 will
360 decrease significantly from acetonitrile to water because the O_2 concentration is reduced by a
361 factor of about 7 (from 1.9×10^{-3} M to 2.7×10^{-4} M in air-saturated solutions at 24°C). This may
362 favor the direct reaction between $^3\text{CT}^*$ and the two volatiles T and linalool for which the
363 water solubility is good and thus the CT photoreduction. In contrast, for 3-carene and α -
364 pinene that show a very low water solubility, CT photoreduction should be insignificant and
365 $^3\text{CT}^*$ could mainly lead to singlet oxygen. However, the lifetime of singlet oxygen is shorter
366 in water (4 μs , Rodgers and Snowden, 1982) than in acetonitrile (61-68 μs , Hurst et al., 1982)
367 which will affect negatively the rate of terpenes photooxidation. Last, the higher polarity of
368 water compared to acetonitrile may increase k_r , although it is already quite high in
369 acetonitrile.

370

371

372 **2.2. Irradiation of CT on thyme's leaves**

373 We started the experiments on thyme's leaves by estimating the amount of CT
374 deposited on two twigs after their dipping in a solution of CT (7.5×10^{-4} M). In the 2 ml of
375 ACN used for the extraction, the CT concentration was of 3.4×10^{-5} M. Based on a total leaves

376 area of 3.6 cm^2 , we finally got a CT concentration of $5 \pm 1 \text{ } \mu\text{g per cm}^2$, which is in the range of
377 the surfacic concentrations calculated for typical CT application rates of $0.5\text{-}1 \text{ kg ha}^{-1}$.

378 Then, CT was irradiated for 6 h in the solar simulator on thyme's leaves or deposited
379 on a glass dish chosen as an inert support and ACN extracts analysed by GC-MS (Figure 4).
380 While no CT photodegradation was observed on dishes, an almost full loss of CT on thyme's
381 leaves was measured. $\text{CT}_{\text{-Cl}}$ and $\text{CT}_{\text{-2Cl}}$ were formed (Inset of Figure 3) confirming the
382 photoreduction of CT when applied on thyme's leaves. T that was present in high amounts in
383 the thyme's twigs was the candidate to induce this photoreduction, even though its
384 involvement in the reaction cannot firmly demonstrated.

385 Moreover, the GC-MS area of T peak increased similarly after 4 h of irradiation for
386 thyme's twigs irradiated in the absence of CT and for thyme's twigs irradiated in the presence
387 of CT from $(2.8 \pm 0.4) \times 10^6$ to $(2.3 \pm 0.9) \times 10^8$ (Table 2). The presence of CT did not affect the
388 nature of T byproducts (TO, TQ, TQO, T-TO_{-2H} and T-TO_{-2H}) and their peak area measured
389 after 4 h of irradiation and in the dark (Table 2). The only evidence of an interaction between
390 CT and T came from the analyses of the gaseous phase of irradiated vials by HS-GC-MS.
391 Indeed, in this case, a drastic loss of T was observed (Figure SI-8). The apparent discrepancy
392 between the HS-GC-MS analyses conducted directly on the volatiles present in the vials and
393 the GC-MS analyses that required extraction of chemicals by ACN can be explained as
394 follows. CT deposited on leaves consumed T present in the gaseous phase, and the weak
395 volatility of T limited any reequilibration through remission from leaves allowing to detect the
396 T loss by HS-GC-MS. However, this T consumption was not measurable after extraction by
397 ACN because extraction allowed the recovering of the great part of T present in the leaves
398 while the loss of T that was related to the initial concentration of CT on the twigs laid below
399 the measurement uncertainties. Indeed, we estimated that 5.7×10^{-7} mole of T could be
400 extracted while 6.7×10^{-8} mole of CT were present on twigs. As one mole of CT was expected

401 to oxidize one mole of T at its best, the amount of T consumed was less than 12% of T
402 extracted, thus negligible.

403 To conclude, we demonstrated that in solution photochemical reactions between CT
404 and thyme's volatiles, in particular T, took place with photoreduction of CT and
405 photooxidation/photochloration of T. On thyme's leaves, photoreduction of CT was also
406 observed. The involvement of T in this reaction was likely based on the data obtained in
407 solution, but could not be firmly confirmed.

408

409 **3. Interactions between IMD and thyme's volatiles**

410 **3.1. Irradiation of IMD and T in acetonitrile solution**

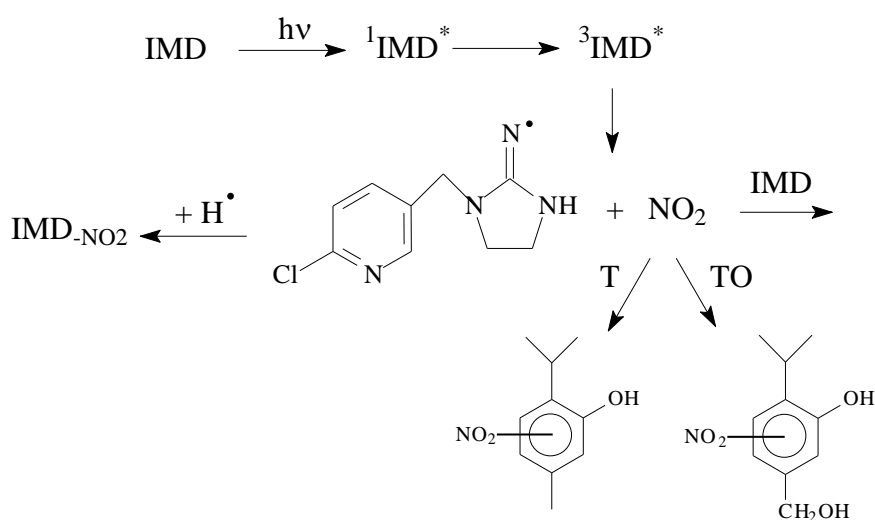
411 After 30 min of irradiation alone in device 2, IMD (10^{-4} M) disappeared by 6.5×10^{-5} M
412 (65%). Three photoproducts were identified (Table 3). The main one gave a peak at $m/z =$
413 211.0742/213.0710 in ES^+ (Figure SI-9) and corresponded to $[M-NO_2+H+H^+]^+$, it was
414 assigned to the imino derivative IMD_{-NO_2+H} . Two other minor peaks were detected at $m/z =$
415 223.0385/225.0356 in ES^- (Figure SI-10) corresponding to $[M-NO-H-H^+]^-$ and at $m/z =$
416 432.0744/434.0715/436.0689 (Figure SI-11) corresponding to $[2M-N_2O_3-H^+]^-$. They were
417 named IMD_{-HNO} and $IMD-IMD_{-N_2O_3}$, respectively.

418 In the presence of T (10^{-3} M), IMD disappeared by 3.0×10^{-5} M (30%) after 30 min of
419 irradiation (Table 4), i. e. less than alone. On the other hand, the T loss was of 7% after 2 h,
420 yielding a consistent consumption of around 1.7×10^{-5} M after 30 min (Table 4). IMD_{-NO_2+H} ,
421 IMD_{-HNO} and $IMD-IMD_{-N_2O_3}$ were detected again but in much smaller amounts than in the
422 absence of T (Table 4). In addition, we detected along TO, a peak at $m/z = 194.0812$ in ES^-
423 (Figure SI-12) corresponding to $[M+NO_2-H-H^+]^-$ and assigned to nitrothymol TNO_2 , a second
424 peak at $m/z = 210.0761$ in ES^- (Figure SI-13) corresponding to $[M+O+NO_2-H-H^+]^-$ assigned to
425 nitrated TO, as well as traces of a peak at $m/z = 358.1649$ in ES^- corresponding to the dimer

426 $[2M+O+NO_2-H-2H-H^+]^-$ and labelled TO-TNO₂. Although solutions were carefully handled
 427 in the dark, traces of TNO₂ were detected in the non-irradiated solutions. It seemed therefore
 428 that IMD was also able to release some NO₂ molecules, spontaneously.

429 These results showed that T inhibited the IMD photodegradation and the
 430 photoproducts formation, in particular that of IMD_{-HNO} and IMD-IMD_{-N₂O₃} while undergoing
 431 nitration. This inhibition strongly suggests that competition between T and IMD took place.

432



433

434 Scheme 5 : Mechanism of IMD photolysis in the presence of T

435

436 As shown in scheme 5, the excitation of IMD released NO₂ by the cleavage of the N-
 437 NO₂ bond and led to the formation of the radical IMD_{-NO₂} that is further converted into IMD.
 438 NO_{2+H} after the abstraction of an H atom (Palma et al., 2020). The formation of TNO₂ could be
 439 explained by the oxidation of T by NO₂ into the corresponding phenoxyl radical followed by
 440 the addition of NO₂ onto it (Marussi and Vione, 2021). Similarly, the nitration of TO into
 441 TONO₂ should involve the oxidation of TO by NO₂ followed by the addition of NO₂ on the
 442 corresponding phenoxyl radical. The lower rate of IMD loss in the presence of T was in favor

443 of a competition between IMD and T for the reaction with NO₂ and suggests that NO₂ reacted
444 with IMD, for example, by H atom abstraction.

445

446 **3.2. Irradiation of IMD on thyme's leaves**

447 As for CT, we estimated the amount of IMD deposited on two twigs after their dipping
448 in a solution of IMD (7.5×10^{-4} M). In the 5 ml of ACN used for the extraction, we measured a
449 IMD concentration of 3.9×10^{-5} M. Based on a total leaves area of 3.6 cm², we finally got a
450 IMD concentration of 14 ± 2 µg per cm² that is enough to observe reactions.

451 Vials containing twigs covered with IMD were irradiated in the solar simulator for 2 h,
452 and in parallel other vials were left in the dark for the control. The ACN extracts were then
453 analyzed by UHPLC-HR-MS. In the samples left in the dark, we detected TO, TNO₂, TONO₂
454 and TO-TNO₂ (Table 4), confirming that the NO₂ release from IMD could also take place in
455 the dark. As shown in Table 4, upon irradiation of IMD on twigs, TNO₂ and TO-TNO₂ were
456 detected in amounts equivalent to those observed in the dark. However, for TONO₂ a 50-
457 folds enhancement was measured. The presence of IMD little increased the formation of TO
458 compared to thyme irradiated in the absence of IMD. Another set of experiments was
459 undertaken on the same variant of thyme just bought in a garden center and thus much
460 younger and much less exposed to solar light. In this case also, nitration reactions were
461 observed under irradiation but they yielded TNO₂ and not TONO₂ as for the older thyme.
462 Accordingly, the young thyme contained much less TO than the older one.

463 Therefore, we conclude that IMD generated nitrocompounds when it was in contact
464 with T, with an increase of the phenomenon under light exposure. The reaction involved the
465 radical NO₂ that was released in the medium mainly photochemically but also spontaneously.
466 T had also an effect of the fate of IMD : by quenching NO₂, it increased its lifetime.

467

468

469 **4. Estimation of the photoproducts toxicities**

470 Using the ECOSAR computer program (version 2.0), we estimated the potential acute
471 (LC_{50}) and chronic toxicity (ChV) of the starting chemicals and their degradation products
472 (Table 5). CT is classified as a moderate toxic chemical. Its photoreduction by T and terpenes
473 in CT_{Cl} and CT_{2Cl} decreases the acute and chronic toxicity on fish from 6.98 to 74.40 $mg L^{-1}$
474 and 0.81 to 7.57 $mg L^{-1}$, respectively and also the bioaccumulation, but these compounds are
475 still classified as moderately toxic compounds. On the other hand, TO is less toxic on fish than
476 T with LC_{50} of 20.90 against 1.86 $mg L^{-1}$ and ChV of 2.08 against 0.21 $mg L^{-1}$ and less
477 bioaccumulated. In contrast, TQ, T- TO_{2H} , TO_{2H} and TCl are more toxic than T with
478 $LC_{50} \leq 1.12 mg L^{-1}$ and $ChV \leq 0.16$. TQ, T- TO_{2H} and TCl are classified as highly toxic. TCl
479 was not detected in the experiments on thyme's leaves, this might be due to a high value of
480 K_{ow} and a diffusion of this compounds inside the cuticle preventing its extraction by ACN. In
481 the case of IMD, T inhibited the pesticide degradation rate and any new chemical deriving
482 from IMD was formed. Other good H-donor chemicals such as phenolic compounds
483 contained in plants may have the same effect and therefore increase the lifetime of IMD and
484 lengthen its insecticidal effect. T and TO underwent nitration. $TONO_2$ is moderately toxic as T
485 with higher LC_{50} but lower ChV, while TNO_2 is classified as highly toxic with $LC_{50} = 1.39$
486 $mg L^{-1}$ and $CHV = 0.15$. Therefore, chemicals that are more toxic than the starting compound
487 can be formed during these reactions.

488

489

490 **Conclusion :**

491 In this work, we investigated the photochemical reactions between pesticides and
492 plant's volatiles in solution and leaf surfaces and we demonstrated that interactions take place

493 in both media. The interactions modified the fate and the transformation pathways of the
494 chemicals and depended on the chemicals structure and the matrix. This was illustrated by the
495 examples of the fungicide chlorothalonil and the insecticide imidacloprid chosen as pesticides
496 and thymol, α -pinene, 3-carene and linalool as plant's volatiles. Studying these reactions is
497 relevant for several reasons. First, they can occur in the real conditions on plants and in
498 surface waters and affecting the fate of the chemicals, these reactions can also alter the
499 phytosanitary treatments shortening the lifetime of the pesticide for example, and lead to
500 repeated and/or increased treatments. These are therefore important factors to consider in the
501 design of pesticides. Secondly, the interactions can potentially generate toxic by-products
502 leading to the pollution of water bodies and of air. The air pollution may be observed in
503 particular in the cities where green roofs are installed. Indeed, their growth in many urban
504 zones in the world could be accompanied by increased possibilities of reactions between
505 plant's volatiles and other chemicals such as the pesticides used to protect the roof plants
506 which might finally lead to an enhanced formation of by-products. For all these reasons, it
507 seems necessary to get a better insight into these overlooked reactions often referred to as
508 « cocktail effect ».

509

510 **Acknowledgments :**

511 This research was supported by a PhD fellowship from the University Clermont-
512 Auvergne/French Ministry of Higher Education and Research. The authors would like to
513 thank Martin Lereboure (Engineer CNRS) and Frédéric Emmenegger (Tech CNRS) for
514 UHPLC-MS analyses, and Guillaume Voyard (Engineer CNRS) for HPLC-DAD analyses.

515

516 **References**

517

518 F. Abbas, Y. Ke, R. Yu, Y. Yue, S. Amanullah. Volatile terpenoids: multiple functions,
519 biosynthesis, modulation and manipulation by genetic engineering. *Planta* (2017) 246, 803–
520 816.
521 doi.org/10.1007/s00425-017-2749-x
522

523 R. Atkinson, J. Arey. Atmospheric Degradation of Volatile Organic Compounds. *Chem. Rev.*
524 (2003) 103, 12, 4605–4638
525 doi.org/10.1021/cr0206420
526

527 R. S. Becker « Theoretical and Interpretation of fluorescence and phosphorescence » Wiley-
528 Interscience, New-York, 1969.
529

530 S. Bouchama, P. de Sainte-Claire, E. Arzoumanian, E. Oliveros, A. Boulkamh, C. Richard
531 Photoreactivity of chlorothalonil in aqueous solution. *Environ Sci Process Impacts* (2014)
532 16(4) 839-847
533 doi.org/10.1039/C3EM00537B
534

535 N. Brand, G. Mailhot, M. Bolte
536 Degradation Photoinduced by Fe(III): Method of Alkylphenol Ethoxylates Removal in Water.
537 *Environ. Sci. Technol.* (1998) 32, 2715–2720
538 doi.org/10.1021/es980034v
539

540 H.D. Burrows, M. Canle L, J.A. Santaballa, S. Steenken. Reaction pathways and mechanisms
541 of photodegradation of pesticides. *J. Photochem. Photobiol. B* (2002) 67, 71-108
542 [doi.org/10.1016/S1011-1344\(02\)00277-4](https://doi.org/10.1016/S1011-1344(02)00277-4)

543

544 F. Chiron, J.C. Chalchat, R.P. Garry, J.F. Pilichowski, J. Lacoste. Photochemical
545 hydroperoxidation of terpenes I. Synthesis and characterization of α -pinene, β -pinene and
546 limonene hydroperoxides. *J. Photochem. Photobiol. A: Chemistry* (1997) 111, 75-86.
547 [doi.org/10.1016/S1010-6030\(97\)00184-6](https://doi.org/10.1016/S1010-6030(97)00184-6)

548

549 N. Dudareva , F. Negre , D. A. Nagegowda, I. Orlova. Plant Volatiles: Recent Advances and
550 Future Perspectives. *Crit Rev Plant Sci* (2006) 25, 417-440
551 doi.org/10.1080/07352680600899973

552

553 A. ter Halle, D. Lavieille, C. Richard. The effect of mixing two herbicides mesotrione and
554 nicosulfuron on their photochemical reactivity on cuticular wax film. *Chemosphere* (2010) 79,
555 482-487
556 doi.org/10.1016/j.chemosphere.2010.01.003Get rights and content

557

558 S. Hamdache, M. Sleiman, P. de Sainte-Claire, F. Jaber, C. Richard. Unravelling the reactivity
559 of bifentazate in water and on vegetables: Kinetics and byproducts. *Sci. Tot. Environ.* (2018)
560 636, 107-114
561 doi.org/10.1016/j.scitotenv.2018.04.219

562

563 A. Hammerbacher, T. A. Coutinho, J. Gershenzon. Roles of plant volatiles in defence against
564 microbial pathogens and microbial exploitation of volatiles. *Plant cell environ.* (2019) 42,
565 2827-2843.
566 doi.org/10.1111/pce13602

567

568 J. R. Hurst, J. D. McDonald, Gary B. Schuster. Lifetime of Singlet Oxygen in Solution
569 Directly Determined by Laser Spectroscopy. *J. Am. Chem. Soc.* 1982, 104, 2065-2067.
570 doi-org.ezproxy.uca.fr/10.1021/ja00371a065
571
572 T. Katagi. Photodegradation of Pesticides on Plant and Soil Surfaces. *Rev Environ Contam*
573 *Toxicol* (2004) 182,1-195.
574 doi.org/10.1007/978-1-4419-9098-3_1
575
576 J.L. Martínez Vidal, P. Plaza-Bolaños, R. Romero-González, A. Garrido Frenich.
577 Determination of pesticide transformation products: A review of extraction and detection
578 methods. *J. Chromat. A* (2009) 1216, 6767-6788
579 doi.org/10.1016/j.chroma.2009.08.013
580
581 G. Marussi, D. Vione. Secondary Formation of Aromatic Nitroderivatives of Environmental
582 Concern: Photonitration Processes Triggered by the Photolysis of Nitrate and Nitrite Ions in
583 Aqueous Solution. *Molecules* (2021) 26, 2550
584 doi.org/10.3390/molecules26092550
585
586 B. Mathon, M. Ferréol, M. Coquery, J.-M. Choubert, J.-M. Chovelon, C. Miège. Direct
587 photodegradation of 36 organic micropollutants under simulated solar radiation: Comparison
588 with free-water surface constructed wetland and influence of chemical structure. *J. Hazard.*
589 *Mat.* (2021) 407, 124801
590 doi.org/10.1016/j.jhazmat.2020.124801
591

592 A. Mellouki, T. J. Wallington, J. Chen. Atmospheric Chemistry of Oxygenated Volatile
593 Organic Compounds: Impacts on Air Quality and Climate. *Chem. Rev.* (2015) 115, 3984–
594 4014
595 doi.org/10.1021/cr500549n
596
597 T. Mochizuki ; F. Ikeda ; A. Tani. Effect of growth temperature on monoterpene emission
598 rates of *Acer palmatum*. *Sci. Tot. Environ.* (2020) 745, 140886
599 doi.org/10.1016/j.scitotenv.2020.140886
600
601 S. Monadjemi, M. el Roz, C. Richard, A. ter Halle. Photoreduction of chlorothalonil fungicide
602 on plant leaf models. *Environ. Sci. Technol.* (2011) 45, 9582-9589
603 doi.org/10.1021/es202400s
604
605 S. L. Murov, I. Carmichael, G. L Hug. Handbook of Photochemistry Second Edition, Marcel
606 Dekker, NY, 1993.
607
608 R. Ossola, O. M. Jönsson, K. Moor, K. McNeill. Singlet Oxygen Quantum Yields in
609 Environmental Waters. *Chem. Rev.* (2021) 121, 4100-4146
610 doi.org/10.1021/acs.chemrev.0c00781
611
612 D. Palma, Y. Arbid, M. Sleiman, P. De Sainte-Claire, C. Richard. New Route to Toxic Nitro
613 and Nitroso Products upon Irradiation of Micropollutant Mixtures Containing Imidacloprid:
614 Role of NO_x and Effect of Natural Organic Matter. *Environ. Sci. Technol.* (2020) 54, 3325–
615 3333
616 [doi.org//10.1021/acs.est.9b07304](https://doi.org/10.1021/acs.est.9b07304)
617

618 S.O. Pehkonen, Q. Zhang. The Degradation of Organophosphorus Pesticides in Natural
619 Waters: A Critical Review. *Crit Rev Environ Sci Technol.* (2002) 32, 17-72.
620 doi.org/10.1080/10643380290813444
621
622 J. Petrović, D. Stojković, M. Soković. Chapter Eight - Terpene core in selected aromatic and
623 edible plants: Natural health improving agents. *Adv. Food Nutr. Res.* (2019) 90, 423-451
624 doi.org/10.1016/bs.afnr.2019.02.009
625
626 J. Porras, J ; J. Fernandez, R. A. Torres-Palma, C. Richard. Humic substances enhance
627 chlorothalonil phototransformation via photoreduction and energy transfer. *Environ. Sci.*
628 *Technol.* (2014) 48, 2218-2225.
629 doi.org/10.1021/es404240x
630
631 S. C. Remke, U. Gunten, S. Canonica. Enhanced transformation of aquatic organic compounds
632 by long-lived photooxidants (LLPO) produced from dissolved organic matter. *Water Res.*
633 (2021) 9, 116707
634 doi.org/10.1016/j.watres.2020.116707
635
636 C. K. Remucal. The role of indirect photochemical degradation in the environmental fate of
637 pesticides: a review. *Environ. Sci.: Processes Impacts* (2014) 16, 628-653
638 doi.org/10.1039/C3EM00549F
639
640 M. A. J. Rodgers, P. T. Snowden. Lifetime of (¹O₂) in Liquid Water As Determined by Time-
641 Resolved Infrared Luminescence Measurements. *J. Am. Chem. Soc.* 1982, 104, 5541-5543.
642 doi-org.ezproxy.uca.fr/10.1021/ja00384a070

643

644 B. Salehi, A. Prakash Mishra, I. Shukla, M. Sharifi- Rad, M. del Mar Contreras, A.
645 Segura- Carretero, H. Fathi, N. Nasri Nasrabadi. Thymol, thyme, and other plant sources:
646 Health and potential uses. *Phytoter Res* (2018) 32, 1688-1706
647 doi.org/10.1002/ptr.6109

648

649 K. Skalska, J.S. Miller, S. Ledakowicz. Trends in NO_x abatement : a review. *Sci. Tot.*
650 *Environ.* (2010) 408, 3976-3989.
651 doi.org/10.1016/j.scitotenv.2010.06.001

652

653 R. M. de Souza, D. Seibert, H.B. Quesada, F. J. Bassetti, M.R. Fagundes-Klen, R.
654 Bergamasco. Occurrence, impacts and general aspects of pesticides in surface water: A
655 review. *Process Saf Environ Prot* (2020) 135, 22-37
656 doi.org/10.1016/j.psep.2019.12.035

657

658 S. Venu, D. B. Naik, S. K. Sarkar, U. K. Aravind, A. Nijamudheen, C. T. Aravindakumar.
659 Oxidation Reactions of Thymol: A Pulse Radiolysis and Theoretical Study. *J. Phys. Chem. A*
660 (2013) 117, 291–299
661 doi.org/10.1021/jp3082358

662

663 D. Vione, C. Minero, F. Housari, S. Chiron. Photoinduced transformation processes of 2,4-
664 dichlorophenol and 2,6-dichlorophenol on nitrate irradiation. *Chemosphere* (2007) 69, 1548–
665 1554
666 doi.org/10.1016/j.chemosphere.2007.05.071

667

668 E.D. Wannaz, J.A. Zygadlo, M.L. Pignata. Air pollutants effect on monoterpenes
669 composition and foliar chemical parameters in *Schinus areira* L. *Sci. Tot. Environ.* (2003)
670 305, 177-193

671 [doi.org/10.1016/S0048-9697\(02\)00466-7](https://doi.org/10.1016/S0048-9697(02)00466-7)

672

673 F. Wilkinson, J.G. Brummer. Rate constants for the decay and reactions of the lowest
674 electronically excited singlet state of molecular oxygen in solution. *J. Phys. Chem. Ref. Data*
675 1981, 10, 809-999.

676 doi.org/10.1063/1.555965

677

678 T. Zeng, W. A. Arnold. Pesticide Photolysis in Prairie Potholes: Probing Photosensitized
679 Processes. *Environ. Sci. Technol.* (2013) 47, 6735–6745

680 doi.org/10.1021/es3030808

681

682

683